

Dynamics of Certain Non-Conformal Degree Two Maps of the Plane

Ben Bielefeld
Scott Sutherland
Folkert Tangerman
Peter Veerman

Introduction

We consider a family of maps which are similar to quadratic maps in that they are degree two branched covers of the Riemann sphere, but not in general conformal. In particular, for α real and fixed, we study maps f_c which are given in polar coordinates by

$$f_c(re^{i\theta}) = r^{2\alpha}e^{2i\theta} + c.$$

For $\alpha = 1$, this is the usual quadratic family ($z \mapsto z^2 + c$), which has been extensively studied and is fairly well understood. For α different from one, f_c is only quasi-conformal, and very different behavior can occur, although there are many strong similarities to the conformal case. It is our goal to determine which results for the quadratic family can be generalized to maps which are topologically similar (and when α is close to 1, close to quadratic), and where such results break down.

In the quadratic family, the orbit of the critical point completely determines the dynamics. This is not the case for the maps f_c : for example, we have found periodic attractors which do not attract the critical point. For certain parameter values, the dynamics is dominated by two dimensional real behavior: periodic saddle points, invariant circles, and so on.

Another striking difference with the quadratic family is the existence of smooth Julia sets. In the conformal case, the only smooth Julia sets are the segment $[-2, 2]$ (for the map $z \mapsto z^2 - 2$) and the unit circle (for the map $z \mapsto z^2$). The corresponding Julia sets for f_c are also smooth, but there are more: we use structural stability techniques to show that for any $\alpha < 1$, the Julia set is C^k -smooth for all c -values sufficiently near 0.

We also study the connectedness locus (the analogue of the Mandelbrot set), and the bifurcations which occur in the c -plane. Numerical evidence strongly suggests that the connectedness locus is always connected, and never locally connected for $\alpha \neq 1$. Furthermore, the bifurcations which occur as the parameter c varies are considerably more complicated than those in the conformal case, although there are many similarities. We discuss these issues at some length in sections 4 and 5.

1: Definitions and Elementary Results

For $\alpha > 0$, consider the map Q_α :

$$Q_\alpha(re^{i\theta}) = r^\alpha e^{i\theta} \quad \text{in polar coordinates}$$

$$Q_\alpha(z) = z^{\frac{\alpha+1}{2}} \bar{z}^{\frac{\alpha-1}{2}} \quad \text{in } (z, \bar{z}) \text{ coordinates, for appropriate branches of the powers}$$

Note that the family $\{Q_\alpha\}$ is a one parameter group: $Q_\alpha \circ Q_\beta = Q_{\alpha\beta}$.

PROPOSITION 1.1. *Each Q_α is a quasi-conformal homeomorphism of the Riemann sphere of constant dilatation $\max(\alpha, 1/\alpha)$.*

For the definition of quasi-conformal, refer to [L].

Proof. Consider $Q = Q_\alpha$. A straightforward computation yields that its dilatation is

$$\text{dil}_Q(z) = \frac{|\partial_z Q| + |\partial_{\bar{z}} Q|}{|\partial_z Q| - |\partial_{\bar{z}} Q|} = \frac{\alpha + 1 + |\alpha - 1|}{\alpha + 1 - |\alpha - 1|} = \max(\alpha, 1/\alpha). \quad \square$$

Denote by P_c the quadratic map on \mathbb{C} : $P_c(z) = z^2 + c$, and let $f_{\alpha,c}$ represent the composition $P_c \circ Q_\alpha$. Then

$$f_{\alpha,c} = \begin{cases} |z|^{2\alpha-2} z^2 + c & \text{or} \\ z^{\alpha+1} \bar{z}^{\alpha-1} + c & \text{in } (z, \bar{z}) \text{ coordinates,} \\ r^{2\alpha} e^{i2\theta} + c & \text{in polar coordinates.} \end{cases}$$

For any $\alpha > 0$ and any $c \in \mathbb{C}$, the map $f_{\alpha,c}$ is a branched cover of \mathbb{C} with a single branch point, the origin, where the map is ramified of degree two. It extends to the Riemann sphere with a branch point at ∞ of degree two. Throughout this paper we always assume that $\alpha > 1/2$. This guarantees that the dynamics near infinity is always the same: the point ∞ is attracting. Moreover, when $\alpha > 1/2$, each $f_{\alpha,c}$ is at least once differentiable everywhere.

For any map $f_{\alpha,c}$, define its *filled-in Julia set* $K(\alpha, c)$ as the set of points whose orbits under $f_{\alpha,c}$ do not accumulate at ∞ . We define the *Julia set* $J(\alpha, c)$ as the the set of points which have no neighborhood in which the iterates of $f_{\alpha,c}$ form an equicontinuous family in the spherical metric. Because $f_{\alpha,c}$ is an open map, the Julia set can be split up into two completely invariant (i.e. forward and backward invariant) subsets $\partial K(\alpha, c)$ and $\Delta(\alpha, c) = J(\alpha, c) - \partial K(\alpha, c)$. In the case when $\alpha = 1$ the set $\Delta(\alpha, c)$ is empty, but in general it is nonempty. For instance, the set $\Delta(\alpha, c)$ may contain stable manifolds of periodic saddle points.

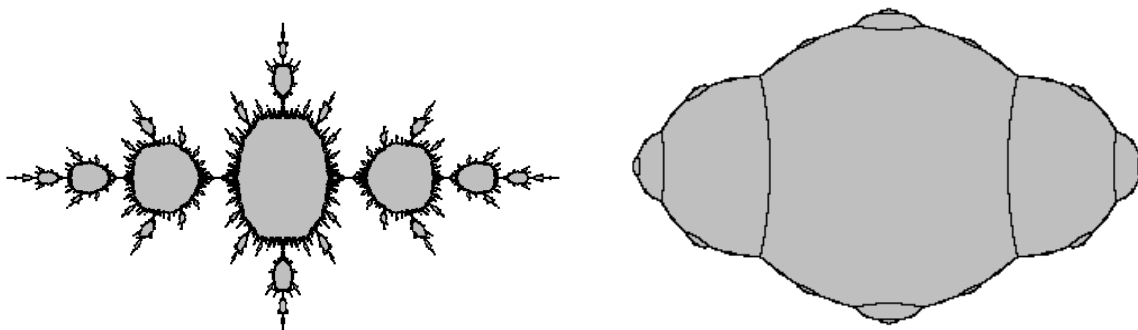


FIGURE 1.2: The filled Julia sets $K(0.75, -0.78)$ and $K(1.5, -0.8)$

PROPOSITION 1.3.

- $K(\alpha, c)$ and $J(\alpha, c)$ are closed and completely invariant.
- $K(\alpha, c)$ and $J(\alpha, c)$ are connected if and only if $0 \in K(\alpha, c)$.
- If $K(\alpha, c)$ is connected, then f is conjugate to the map $z \mapsto z^2$, $|z| > 1$ on the complement of $K(\alpha, c)$.

Proof. The proof is essentially the same as the proof for quadratic polynomials. Refer to [DH], [Bl], or [M]. \square

PROPOSITION 1.4. *Every path component of $K(\alpha, c)$ is simply connected.*

Proof. If γ is a Jordan curve contained in $K(\alpha, c)$, then its iterates are bounded. Consider the component D of $\mathbb{C} - \gamma$ which does not contain infinity. Since $f_{\alpha, c}: \mathbb{C} \rightarrow \mathbb{C}$ is an open map, a point in D cannot map to a boundary point of $f^n(D)$ under f^n . Thus $\partial f^n(D) \subset f^n(\partial D) = f^n(\gamma)$, and $f^n(D)$ will then be bounded. Therefore D is contained in $K(\alpha, c)$. \square

Define for fixed α the *connectedness locus* \mathcal{C}_α of the family $\{f_{\alpha, c}\}_{c \in \mathbb{C}}$ as

$$\mathcal{C}_\alpha = \{c \mid K(\alpha, c) \text{ is connected}\}$$

The set \mathcal{C}_1 is known as the Mandelbrot set. An interesting issue is the dependence of \mathcal{C}_α on the parameter. An isolated saddle-node bifurcation which results in an attractor which attracts the critical point could ruin the continuity in the Hausdorff topology. We have not observed such a bifurcation. At this point we formulate the following conjecture:

CONJECTURE 1.5. *The connectedness locus \mathcal{C}_α varies continuously with α in the Hausdorff topology.*

There is another set of points \mathcal{D}_α in the parameter space that is interesting,

$$\mathcal{D}_\alpha = \{c \mid K(\alpha, c) \text{ is not totally disconnected}\}.$$

In the conformal case, $K(\alpha, c)$ is not connected if and only if it is totally disconnected. In section 2, we show that for large c the set $K(\alpha, c)$ is totally disconnected. In the case where $\alpha < 1$, there are c values for which $K(\alpha, c)$ is not connected and not totally disconnected (see section 4). It may be that for $\alpha \geq 1$ that $\mathcal{C}_\alpha = \mathcal{D}_\alpha$. This is about all we know about \mathcal{D}_α . It would be interesting to find a computer algorithm to draw this set.

Besides the Mandelbrot set (\mathcal{C}_1), the two extreme examples can be fairly well understood.

PROPOSITION 1.6. *The connectedness locus $\mathcal{C}_{1/2}$ is a union of half lines, containing the origin.*

Proof. Let f_c denote the map $f_{1/2, c}$. Then for any $k > 0$,

$$f_{kc}(kz) = kf_c(z).$$

Consider the orbit of the critical point. It is easily seen by induction that $f_{kc}^{n+1}(0) = kf_c^{n+1}(0)$. Therefore, the property that the orbit of the critical point be bounded is independent of k . \square

PROPOSITION 1.7. *As $\alpha \rightarrow \infty$, \mathcal{C}_α converges in the Hausdorff topology to the unit disk.*

Proof. Note that for $|c| > 1$ and α large enough, $f_{\alpha,c}^2(0)$ is close to infinity. Consequently, any Hausdorff limit is contained in the closed unit disk. On the other hand, when $|c| < 1$, and ϵ is small, then for α large enough, the orbit of the critical point is contained in the disk of radius $|c| + \epsilon$. Therefore, any open disk contained in the closed unit disk is contained in \mathcal{C}_α for α large enough. \square

In the following sections we describe some theorems, conjectures, and numerical results.

2: When Disconnected Filled-in Julia Sets are Cantor Sets

In the holomorphic case ($\alpha = 1$), filled-in Julia sets are totally disconnected when they are disconnected. When $\alpha \neq 1$, this need no longer be true. One can find values of the parameter for which there are periodic attractors, while the critical point tends to ∞ . These examples have only been found when $\alpha < 1$ (see section 4). On the other hand, when α is fixed and $|c|$ is large enough, this cannot occur.

THEOREM 2.1. *Let α be fixed, and $|c| - |2c|^{1/2\alpha} \geq 1$, then $K(\alpha, c)$ is totally disconnected, $K(\alpha, c) = J(\alpha, c)$ and $f_{\alpha,c}|_{J(\alpha,c)}$ is uniformly expanding.*

Proof. The idea of our proof of this theorem is straightforward. First, we show in the lemma below that there is a disk containing the critical point which iterates to ∞ . The next proposition shows that the map on the filled-in Julia set is uniformly expanding; the theorem follows immediately. \square

LEMMA 2.2. *If $|c| \geq 2^{\frac{1}{2\alpha-1}}$, then*

$$\left(|c| - |2c|^{1/2\alpha}\right)^{1/2\alpha} \leq |z| \leq |c|$$

for any $z \in K(\alpha, c)$.

Proof. When $|c| \geq 2^{\frac{1}{2\alpha-1}}$, we have $|c|^{2\alpha} \geq 2|c|$. Consider a point z with $|z| > |c|$. Then

$$\begin{aligned} |f_{\alpha,c}(z)| &\geq |z|^{2\alpha} - |c| \\ &= (|z/c|^{2\alpha})|c|^{2\alpha} - |c| \\ &> |z/c|(2|c|) - |c| \\ &= 2|z| - |c| \\ &> |z|. \end{aligned}$$

If the orbit of z remains bounded, then by continuity of f there is a limit point z_∞ of the orbit such that $|f_{\alpha,c}(z_\infty)| = |z_\infty|$, yielding a contradiction. Therefore, the orbit of z goes to infinity, and so $z \notin K(\alpha, c)$.

On the other hand suppose $|z| < (|c| - |2c|^{1/2\alpha})^{1/2\alpha}$. We show that the second iterate of z is outside the disk of radius $|c|$, and hence by the above argument, the orbit of z goes to infinity. We have

$$\begin{aligned} |f_{\alpha,c}(f_{\alpha,c}(z))| &\geq |f_{\alpha,c}(z)|^{2\alpha} - |c| \\ &\geq \left| |c| - |z|^{2\alpha} \right|^{2\alpha} - |c| \\ &> (|2c|^{1/2\alpha})^{2\alpha} - |c| \\ &= |c|. \end{aligned} \quad \square$$

COROLLARY 2.3.

- If $|c| > 2^{\frac{1}{2\alpha-1}}$ then $0 \notin K(\alpha, c)$ and thus $c \notin \mathcal{C}_\alpha$.
- If $c \in \mathcal{C}_\alpha$ and $z \in K(\alpha, c)$, then $|c| \leq 2^{\frac{1}{2\alpha-1}}$ and thus $|z| \leq 2^{\frac{1}{2\alpha-1}}$.

PROPOSITION 2.4. *If $|c| - |2c|^{1/2\alpha} \geq 1$, then $f_{\alpha,c}$ expands the Euclidean metric on $K_{\alpha,c}$.*

Proof. Let f denote $f_{\alpha,c}$, let z be a point in $K_{\alpha,c}$, let A denote $D_z f$, and let v be a non-zero tangent vector in $T_z \mathbb{C}$. We must show that $\langle Av, Av \rangle > \langle v, v \rangle$, or equivalently $\langle A^* Av, v \rangle > \langle v, v \rangle$. Since $A^* A$ has an orthonormal basis of eigenvectors with positive eigenvalues, it suffices to show that the minimum eigenvalue λ_{\min} of $A^* A$ is greater than 1.

For general f we have $\lambda_{\min} = (|f_z| - |f_{\bar{z}}|)^2$, and in our case $\lambda_{\min} = (\alpha + 1 - |\alpha - 1|)^2 |z|^{4\alpha-2}$. By Lemma 2.2, we have $|z| \geq (|c| - |2c|^{1/2\alpha})^{1/2\alpha} \geq 1$, since $z \in K_{\alpha,c}$. When $\alpha \geq 1$,

$$\lambda_{\min} = 4|z|^{4\alpha-2} \geq 4,$$

and when $1/2 < \alpha \leq 1$,

$$\lambda_{\min} = 4\alpha^2 |z|^{4\alpha-2} \geq 4\alpha^2 > 1. \quad \square$$

3: Smooth Julia Sets

In the holomorphic case there are only two smooth Julia sets. When $c = 0$, the Julia set is the unit circle, and in this case the Julia set is hyperbolic. When the critical value c is real and is one of the preimages of a repelling fixed point, then the Julia set is the closed interval between $-|c|$ and $|c|$. This value for c is at the ‘‘tip of the Mandelbrot set’’, and in this case the dynamics on the Julia set is sub-hyperbolic (i.e. the dynamics on this Julia set is expanding with respect to a metric which is smoothly equivalent to the Euclidean metric except at a finite number of points.)

For fixed values of α , one finds readily the parameter value for which the critical value is a preimage of a repelling fixed point. This fixed point is real and has coordinate $-c$. The fixed point equation is

$$|c|^{2\alpha} + c = -c$$

Consequently, $c = -2^{1/(2\alpha-1)}$. Let us denote the corresponding Julia set by J_α . Numerical observations suggest that when α is between $1/2$ and 2 , J_α is indeed an interval, and that when α is greater than 2 , J_α is not contained in the real line.

THEOREM 3.1. *When α is between 0.5 and 1.7, the Julia set J_α consists of an interval. The dynamics on J_α is sub-hyperbolic.*

The idea of the proof is straightforward: to find a metric which is contracted by the inverse (branches) of $f = f_{\alpha, c_\alpha}$. Consider the metric

$$\rho_\alpha(z)|dz| = \frac{|dz|}{|c^2 - z^2|^{\frac{2\alpha-1}{2\alpha}}}$$

The restriction of this metric to the interval $[-c, c]$ was considered by Jiang [J1].

PROPOSITION 3.2. *When $0.5 \leq \alpha \leq 1.7$, then f expands the metric ρ_α on the ball of radius $\frac{1}{2^{2\alpha-1}}$.*

Proof. We want to show that $f^*(\rho_\alpha) > \rho_\alpha$. We let $p = \frac{2\alpha-1}{2\alpha}$. We note that $2c = -|c|^{2\alpha}$ and $f(z) = z^{\alpha+1}\bar{z}^{\alpha-1} + c$.

$$\begin{aligned} f^*(\rho_\alpha)(z) &= \frac{|f_z dz + f_{\bar{z}} d\bar{z}|}{\left|c^2 - (|z|^{2\alpha-2} z^2 + c)^2\right|^p} \\ &= \frac{|(\alpha+1)\bar{z}^{\alpha-2} z^\alpha \bar{z} dz + (\alpha-1)\bar{z}^{\alpha-2} z^\alpha z d\bar{z}|}{\left|2c|z|^{2\alpha-2} z^2 + z^4 |z|^{4\alpha-4}\right|^p} \\ &= \frac{|(\alpha+1)dz + (\alpha-1)\frac{z}{\bar{z}} d\bar{z}|}{|z|^{1-2\alpha} \left|z|^{4\alpha-4} z^4 - |c|^{2\alpha} |z|^{2\alpha-2} z^2\right|^p} \\ &= \frac{|(\alpha+1)dz + (\alpha-1)\frac{z}{\bar{z}} d\bar{z}|}{\left||z|^{2\alpha-2} z^2 - |c|^{2\alpha}\right|^p} \end{aligned}$$

We now wish to show that the “expansion” ratio $f^*(\rho_\alpha)/\rho_\alpha$ at a point z in the disk of radius $\frac{1}{2^{2\alpha-1}}$ is bounded from below by one. We have

$$\frac{f^*(\rho_\alpha)}{\rho_\alpha} = \left|(\alpha+1) + (\alpha-1)\frac{z}{\bar{z}}\frac{d\bar{z}}{dz}\right| \left(\frac{|c^2 - z^2|}{\left||c|^{2\alpha} - |z|^{2\alpha-2} z^2\right|}\right)^p$$

Now let $z = 2^{\frac{1}{2\alpha-1}} x e^{i\theta}$. Since z is in the closed disk of radius $2^{\frac{1}{2\alpha-1}} = |c|$, we have $0 \leq x \leq 1$. Denote by $e^{i\phi}$ the quantity $d\bar{z}/dz$. We can express the expansion ratio as the product of two terms. The first is

$$|(\alpha+1) + (\alpha-1)e^{i(2\theta+\phi)}|$$

which is bounded below by 2α when $\alpha \leq 1$ and by 2 when $\alpha \geq 1$. The second term is

$$\left(\frac{|2^{\frac{2}{2\alpha-1}}(1 - e^{2i\theta} x^2)|}{|2^{\frac{2\alpha}{2\alpha-1}}(1 - e^{2i\theta} x^{2\alpha})|}\right)^p = 2^{\frac{1-\alpha}{\alpha}} \left(\frac{|1 - e^{2i\theta} x^2|}{|1 - e^{2i\theta} x^{2\alpha}|}\right)^p.$$

Notice that

$$\frac{|1 - e^{2i\theta}x^2|}{|1 - e^{2i\theta}x^{2\alpha}|} > \begin{cases} 1/\alpha & \text{when } \alpha > 1, \\ 1/2 & \text{when } \alpha \leq 1. \end{cases}$$

Hence for $\alpha > 1$, the expansion factor is greater than $2^{1/\alpha}(1/\alpha)^{\frac{2\alpha-1}{2\alpha}}$, which is a decreasing function of α and is bigger than 1 for all $\alpha \in [1, 1.7]$. For $\alpha < 1$, the expansion factor is greater than $\alpha 2^{\frac{3-2\alpha}{2\alpha}}$, which is also a decreasing function of α , and is greater than 1 when $\alpha = 1$. We conclude that when $1/2 \leq \alpha \leq 1.7$, the ratio $f^*(\rho_\alpha)/\rho_\alpha$ is uniformly greater than one for all points z within the disk of radius $2^{\frac{1}{2\alpha-1}}$. \square

With this fact in hand, we can now prove Theorem 3.1.

Proof. By Corollary 2.3, the filled-in Julia set is contained in the closed disk D of radius $2^{\frac{1}{2\alpha-1}}$. From the proof of Lemma 2.2, it follows that the inverses of f map this disk into itself. Let S_0 and S_1 be the two components of the inverse image of the disk.

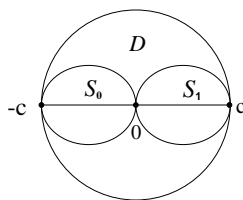


FIGURE 3.3: The disk D and its inverse images S_0 and S_1

The two inverse branches $\psi_i: D \rightarrow S_i$ are homeomorphisms; by the previous proposition, they are uniformly contracting. Thus, the diameter of the sets $\psi_{\epsilon_1} \circ \psi_{\epsilon_2} \circ \dots \circ \psi_{\epsilon_n}(D)$ go to 0 geometrically. Hence, there is exactly one point x_ϵ with the n^{th} iterate of x_ϵ in S_{ϵ_n} , where $\epsilon = (\epsilon_1, \epsilon_2, \dots)$ (preimages of the critical value have two such representations ϵ). For each ϵ there is a point on the real segment with the itinerary ϵ , and so there are no other points in the filled-in Julia set. \square

CONJECTURE 3.4. *For all α in $(1/2, 2)$, the Julia set J_α is the interval $\left[-2^{\frac{1}{2\alpha-1}}, 2^{\frac{1}{2\alpha-1}}\right]$, and the dynamics on J_α is sub-hyperbolic.*

Structural Stability. We now investigate structurally stable properties for α fixed and c near zero. Consider $f_c = f_{\alpha,c}$. Take c to be zero. The unit circle S^1 is smooth, f_0 -invariant and repelling. In fact $T_{S^1}\mathbb{C}$ splits as a direct sum of invariant bundles N , the radial direction, and TS^1 :

$$T_{S^1}\mathbb{C} = TS^1 \oplus N.$$

When $v \in TS^1$, $|Df_0(v)| = 2|v|$, while when $v \in N$, $|Df_0(v)| = 2\alpha|v|$. Let $m = \frac{\ln(2\alpha)}{\ln 2}$, then the dynamics near S^1 is m -normally hyperbolic in the sense of Hirsch-Pugh-Shub [HPS].

On $\mathbb{C} - \{0\}$, we have the foliation by concentric circles and the foliation by radial lines. These foliations are invariant (i.e. every component of f_0^{-1} of a leaf is contained in a leaf), smooth, and intersect transversly. We consider the stability properties of these foliations.

DEFINITION. Let A be an annulus. A foliation on A is *circular* if each of the boundary components of A are leaves and if every leaf is homeomorphic to a circle. A foliation on A is *transverse* if every leaf is homeomorphic to a closed interval and intersects each of the boundary components of A in a single point. We say that a circular (transverse) foliation on A is C^k when each leaf is C^k -diffeomorphic to a round circle (interval) and when nearby leaves are C^k -close.

Let A and B be domains in the plane. Let $f : B \rightarrow A$ be a smooth nonsingular map. Then any foliation on A lifts to a foliation on B . We say that a (C^k) foliation on A is *compatible with the dynamics* if it and its lift to B form a (C^k) foliation of $A \cup B$.

Consider a concentric annulus A containing S^1 . Then $f_0^{-1}(A)$ is strictly contained in A . Choose a circular foliation on $A_0 = A - f_0^{-1}(A)$ which is C^k -close to the foliation by round circles (in particular, transverse to the radial foliation). We can obtain a foliation on $A - S^1$ by repeatedly pulling back by f_0^{-1} ; adding S^1 gives an f_0 -invariant foliation A whose leaves are Jordan curves.

One easily shows that every leaf of this foliation is a graph of radial function $(r(\theta), \theta)$; these graphs are uniformly C^k for all $k \leq \frac{\ln(2\alpha)}{\ln 2}$. The leaves on $A_n = A - f_0^{-n-1}(A)$ converge to the round circle in the C^k topology.

Next, consider a transverse foliation of $A - f_0^{-1}(A)$ by smooth arcs, running from one boundary component to another in each component annulus, which is transverse to the foliation by round circles and compatible with the dynamics. Pull back by the dynamics to obtain a foliation of $A - S^1$ by smooth curves which is transverse to the circular foliation. Since f_0^{-1} is a contraction, each of these curves limits on S^1 , and at least two curves land at each point of S^1 (one from the inside and one from the outside). Moreover, each of these curves is an angular graph $(r, \theta(r))$ and is uniformly C^k for all $k \leq \frac{\ln 2}{\ln(2\alpha)}$. If $\alpha < 1$, the resulting foliation extends to all of A and all leaves are uniformly C^k for all $k < m$. However, if $\alpha > 1$ and the initial foliation is not exactly radial, the curves can not meet smoothly at S^1 .

THEOREM 3.9. Fix $\alpha \neq 1$ and a concentric annulus A containing the unit circle in its interior, and let $m = \frac{\ln(2\alpha)}{\ln 2}$.

- If $\alpha > 1$, then for all $k < m$ there exists δ_k so that when $|c| < \delta_k$, any initial circular C^k foliation on $A - f_c^{-1}(A)$ which is close to the round foliation will pull back and extend to an f_c -invariant C^k foliation on A .
- If $\alpha < 1$, then for all $k < 1/m$ there exists δ_k so that when $|c| < \delta_k$, any C^k transverse foliation on $A - f_c^{-1}(A)$ which is close to the radial foliation and dynamically compatible, will pull back and extend to an f_c -invariant C^k foliation on A .

COROLLARY 3.10.

- If $\alpha > 1$ and $|c| < \delta_k$, the Julia set $J(\alpha, c)$ is a C^k curve.
- If $\alpha < 1$ and $|c| < \delta_k$, the Julia set $J(\alpha, c)$ intersects every leaf of the corresponding radial foliation in a single point.

DYNAMICS OF CERTAIN NON-CONFORMAL MAPS OF \mathbb{C}

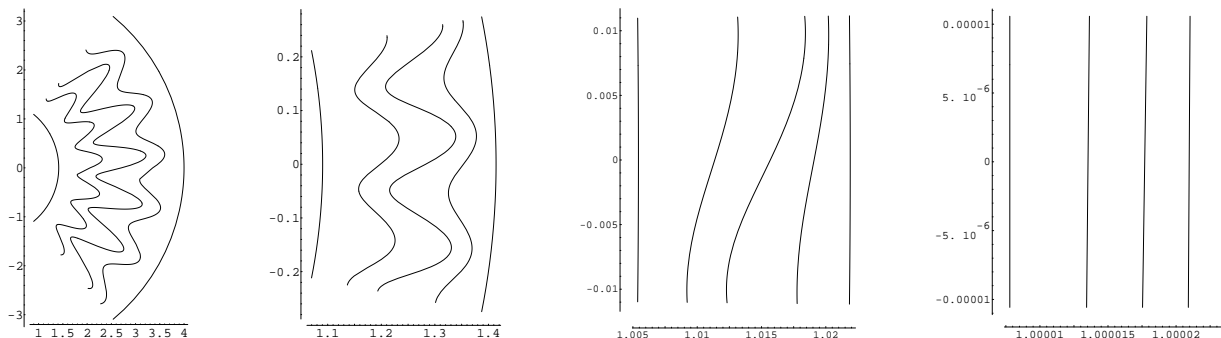


FIGURE 3.5: Part of several leaves of a circular foliation on the outer component of A_0 , and the pullbacks to A_1 , A_3 , and A_8 when $\alpha = 2$. These leaves converge to the round circle in the C^2 topology.

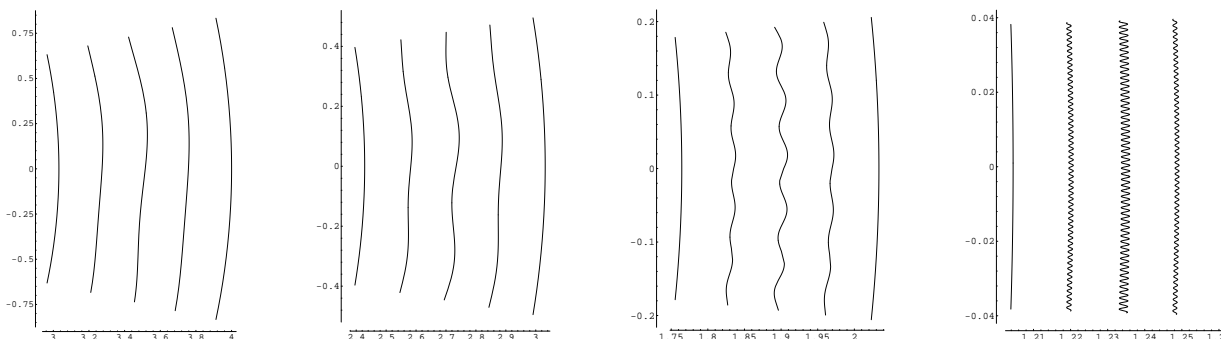


FIGURE 3.6: Leaves of a circular foliation on the outer component of A_0 , and pullbacks to A_1 , A_3 , and A_8 when $\alpha = 5/8$. The convergence to the circle is only C^0 .

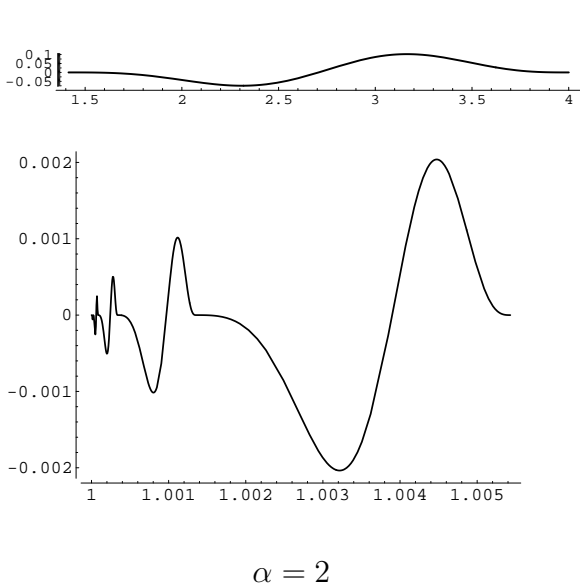


FIGURE 3.7: Above, we show a leaf of a transverse foliation on the outer component of A_0 which is close to the radial one. Below is a leaf of the corresponding foliation on the outer component of $\bigcup_{n=3}^{\infty} A_n$ when $\alpha = 2$; notice the lack of smoothness near the limit at $(1, 0)$.

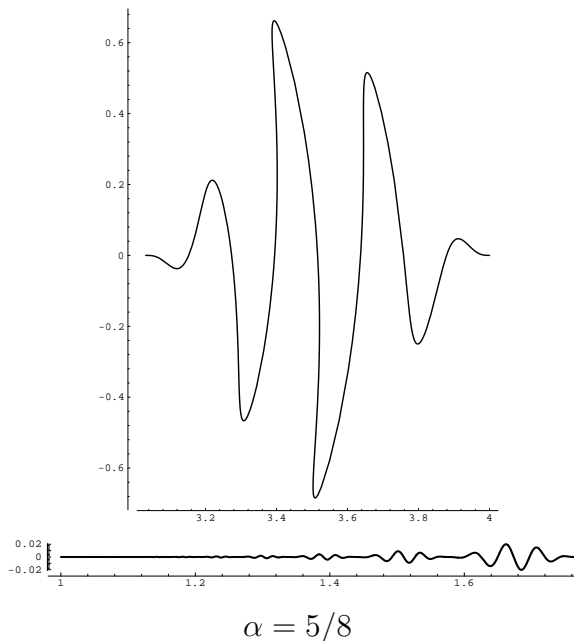


FIGURE 3.8: As on the left, we have a leaf of the initial foliation above and a leaf of the induced foliation below. Even though the initial foliation is quite far from the radial one, as it approaches S^1 the C^3 limit of the resulting leaf is exactly radial.

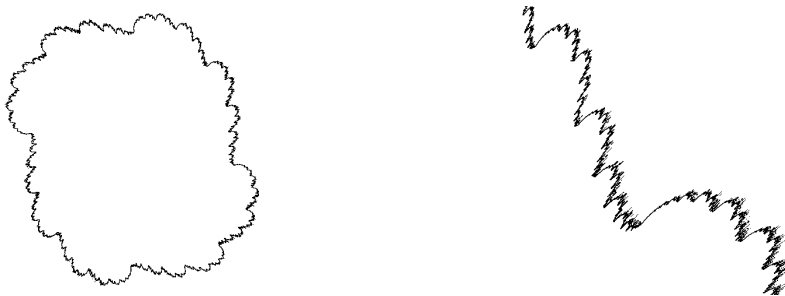


FIGURE 3.11: The Julia set for $\alpha = .75, c = .1 + .1i$, and a blowup of it. This illustrates Corollary 3.10: although the Julia set is not at all smooth, it looks like the graph of a polar function $r = f(\theta)$.

Proof. Most of the technical details can be found in [HPS] (diffeomorphisms). Since the maps we discuss here have degree 2, the initial setup is a little bit different. Consider the following cone fields on $\mathbb{C} - \{0\}$:

$$C^+(r, \theta) = \left\{ R \frac{\partial}{\partial r} + \Theta \frac{\partial}{\partial \theta} \mid |R| \leq |\Theta| \right\}$$

$$C^-(r, \theta) = \left\{ R \frac{\partial}{\partial r} + \Theta \frac{\partial}{\partial \theta} \mid |R| \geq |\Theta| \right\}$$

When $\alpha > 1$, f_0^{-1} maps C^+ strictly into itself. Consider the annulus A . For $|c|$ small enough, f_c^{-1} maps the cone field C^+ on A strictly into itself. Choose an initial circular foliation on $A_0 = A - f_c^{-1}(A)$ where the tangent vectors at each point are in the cone C^+ , and extend this to a foliation \mathcal{F}_0 on all of A which has the same property. Define a new foliations \mathcal{F}_1 as follows: pull back \mathcal{F}_0 on A_0 by f_c^{-1} to obtain a foliation on $A_1 = A - f_c^{-2}(A)$. Extend this to all of A as before to obtain \mathcal{F}_1 . We iterate this procedure to obtain a sequence of circular foliations \mathcal{F}_n on A .

Now choose $k < m$, and assume that the leaves of \mathcal{F} are C^k . The techniques in [HPS] show that when $|c|$ is small enough, the sequence \mathcal{F}_n is C^k -compact and therefore has a limit point \mathcal{F}_∞ which only depends on the choice in $A - f_c^{-1}(A)$. Since the foliations \mathcal{F}_n agree on larger and larger domains, \mathcal{F}_∞ is the only limit point. In particular, the Julia set $J(\alpha, c)$ is C^k .

When $\alpha < 1$, the situation is reversed: the cone field C^- is mapped into itself by f_0^{-1} . When $|c|$ is sufficiently small, f_c^{-1} maps C^- restricted A into itself. Now consider a transverse foliation on $A - f_c^{-1}(A)$ which is dynamically compatible and whose tangent-line field is in the cone field C^- . Extend this foliation to all of A so that the tangent-line field is in the cone field everywhere. We now repeat the pull-back construction. When $k < \frac{1}{m}$ we now have a C^k -compact sequence of transverse foliations on A , for $|c|$ sufficiently small. And again, there is a single limit point which only depends on the initial choice in $A - f_c^{-1}(A)$.

We finally argue that the Julia set intersects every leaf in exactly one point. The Julia set $J(\alpha, c)$ certainly intersects every leaf in at least one point. If it intersects in say two points, we can iterate forward and conclude that there are points of the Julia set in $A - f_c^{-1}(A)$. This is a contradiction. \square

a periodic attractor of period q , then at each point of the boundary of this component one has a neutral periodic cycle and, taking the q^{th} iterate, reduces the study of the bifurcation to that of the Leau bifurcation. In particular the boundary of such a component is an algebraic curve.

When $\alpha \neq 1$ our understanding is already incomplete for the period one component, which we define as the set of parameters c in the connectedness locus for which $f_{\alpha,c}$ has an attracting fixed point. Moreover, the analysis we carry out in the period one component does not automatically extend to the components corresponding to periodic attractors of higher period. We show below that when $\alpha \neq 1$ and an attractor is present, the critical point is not necessarily attracted to it.

Fix α . We first analyze the fixed point picture. Note that for every z_0 there is a c such that z_0 is a fixed point of $f_{\alpha,c}$, namely $c = z_0 - z_0^{\alpha+1}\bar{z}_0^{\alpha-1}$. If z_0 is a fixed point of $f_{\alpha,c}$, the derivative $D(z_0)$ of $f_{\alpha,c}$ at z_0 is

$$(\alpha + 1)z_0^\alpha\bar{z}_0^{\alpha-1}dz + (\alpha - 1)z_0^{\alpha+1}\bar{z}_0^{\alpha-2}d\bar{z}.$$

The point z_0 is an attracting fixed point if the eigenvalues of $D(z_0)$ are both in the unit disk. In the closure of the set of such attracting fixed points, there are three important curves:

- The curve δ where the determinant of $D(z_0) = 1$.
- The curve γ_+ where $D(z_0)$ has an eigenvalue of $+1$.
- The curve γ_- where $D(z_0)$ has an eigenvalue of -1 .

A point $z_0 = r_0e^{i\theta_0}$ is on δ if and only if

$$\det D(z_0) = 4\alpha r_0^{4\alpha-2} = 1,$$

and therefore δ is a circle of radius $(4\alpha)^{\frac{1}{2-4\alpha}}$.

A point z_0 is on γ_+ if and only if

$$1 - \text{tr}(D(z_0)) + \det(D(z_0)) = 0$$

or equivalently,

$$1 - 2(\alpha + 1)r_0^{2\alpha-1}\cos(\theta_0) + 4\alpha r_0^{4\alpha-2} = 0.$$

We claim that γ_+ is a smooth simple closed curve. This equation has at most two roots $r_0^{2\alpha-1}$. Because we want to only consider the solutions for r_0 positive, we must have $\cos\theta_0 \geq 0$. Moreover, the discriminant of this equation is non-negative for $\cos^2(\theta_0) > 4\alpha/(\alpha+1)^2$, that is, in an angular sector about the real axis (when $\alpha = 1$, this sector reduces to a single point) and the discriminant vanishes at the ends of that angular sector. Consequently, γ_+ is a topological circle. One can check that the curve is C^1 ; we leave that to the reader.

The curve γ_+ intersects the curve δ in two points (one when $\alpha = 1$). Notice that

$$\gamma_- = -\gamma_+$$

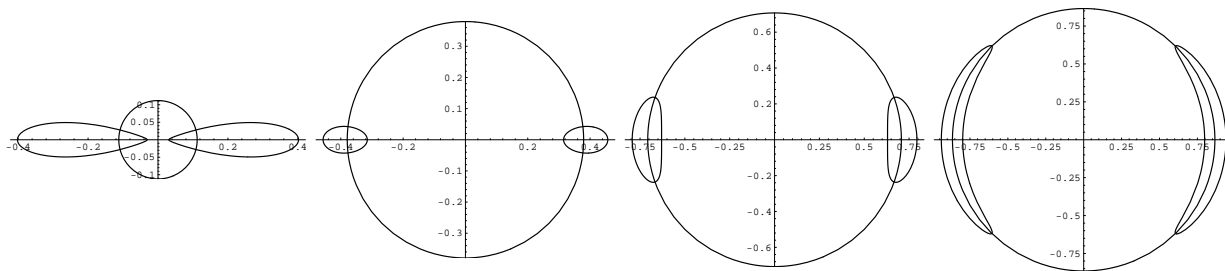


FIGURE 4.1: The curves δ , γ_+ , and γ_- for $\alpha = .6$, $\alpha = .8$, $\alpha = 2$, and $\alpha = 6$.

because z_0 is on γ_- if and only if $1 + \text{tr}(D(z_0)) + \det(D(z_0)) = 0$.

Define

$$P_1(\alpha) = \{c \mid f_{\alpha,c} \text{ has an attracting fixed point}\}.$$

The previous analysis immediately provides us with insight about $P_1(\alpha)$. Consider the map $p : \mathbb{C} \rightarrow \mathbb{C}$ which assigns to each z the parameter value c for which z is a fixed point of f_c :

$$f_{p(z)}(z) = z$$

One obtains that

$$p(z) = z - z^{\alpha+1} \bar{z}^{\alpha-1}.$$

When z is real, $p(z)$ is real and p commutes with conjugation. One checks that p is injective on γ_{\pm} , injective on δ when $\alpha \geq 1$, and has a single point of multiplicity 2 on δ when $\alpha < 1$.

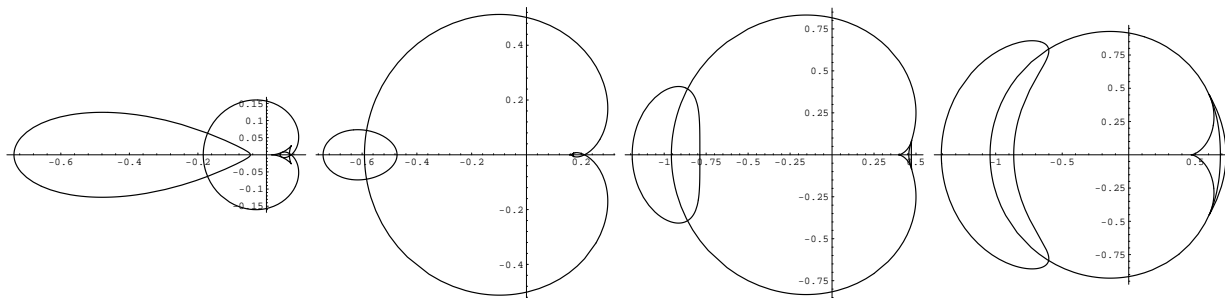


FIGURE 4.2: The curves $p(\delta)$, $p(\gamma_+)$, and $p(\gamma_-)$ $\alpha = .6$, $\alpha = .8$, $\alpha = 2$, and $\alpha = 6$.

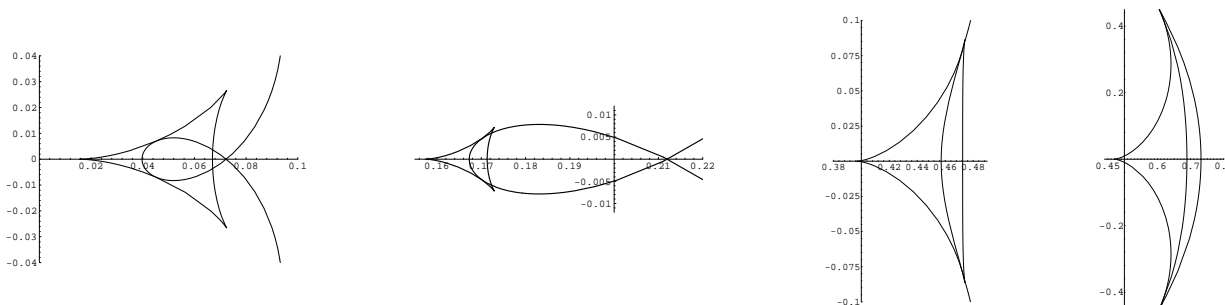


FIGURE 4.3: A blowup of Figure 4.2 near $p(\gamma_+)$.

We will now discuss the dynamics of the fixed points $z_0 \in p^{-1}(c)$ for c in \mathbb{C} . We present the outcome first, followed by a partial analysis. The bifurcations occur as you pass through the curves $p(\gamma_{\pm})$ and $p(\delta)$. One can show that, for $\alpha \neq 1$, $p(\delta)$ is a limaçon, $p(\gamma_-)$ is diffeomorphic to a circle, and that $p(\gamma_+)$ is a simple closed curve with three cusps.

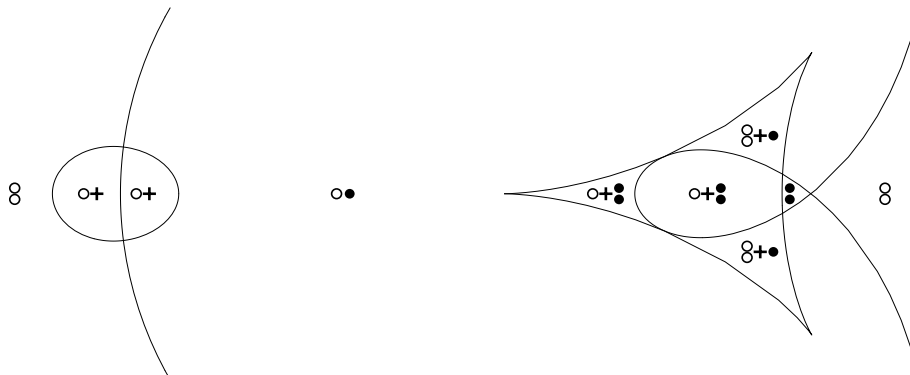


FIGURE 4.4: The types of fixed points occurring in the c -plane when $1/2 < \alpha < 1$. Each region is labelled by symbols indicating the types of fixed points which exist there: a symbol \bullet is used for each attracting fixed point, \circ for each repelling fixed point, and $+$ for each saddle. For example, in the region marked $\circ+$, there is exactly one repelling fixed point, one saddle, and no attracting fixed point. The upper and lower portions of the limaçon $p(\delta)$ have been omitted, and the region on the right side has been greatly magnified.

CASE $1/2 < \alpha < 1$ (Figure 4.4): In this case the limaçon $p(\delta)$ has an inner loop. In this case, there can be attracting fixed points which fail to attract the critical point.

Region $\textcircled{8}$ Outside the limaçon $p(\delta)$ and outside $p(\gamma_-)$, there are always two repelling fixed points.

Region $\circ+\bullet$: Inside $p(\gamma_+)$ there are 4 components cut out by the limaçon. Region $\circ+\bullet$ is given by the two pieces which intersect the real line. There are two attracting points, one repelling point, and one saddle. Part the curve $p(\delta)$ crosses this region, but crossing this curve only changes the product of the eigenvalues of the saddle from less than one to greater than one; no bifurcation occurs.

Region $\textcircled{8}+\bullet$ This region consists of the two components inside $p(\gamma_+)$ which do not intersect the real line; here there is one attracting fixed point, a saddle, and two repelling fixed points. Crossing the curve $p(\delta)$ into region $\circ+\bullet$ causes one of the repelling points to undergo a Hopf bifurcation (see below) and become attracting. As one crosses the curve $p(\gamma_+)$ into the $\circ\bullet$ region, a saddle and repelling fixed point collide and cancel each other.

Region \bullet : Outside $p(\gamma_+)$ but inside the inner loop of the limaçon, we have two attracting fixed points. When one crosses $p(\delta)$ into region $\circ\bullet$, one of the attracting points becomes a repelling point, generally with a Hopf bifurcation. Entering this region from $\circ+\bullet$ causes the repelling point and the saddle to cancel each other. We note that since there are two attracting fixed points, there must be at least one which doesn't attract the critical point. In fact, when c is real the critical point iterates to infinity.

Region $\circ+$ Inside $p(\gamma_-)$, there is always one repelling fixed point and one saddle. As above, the part of the $p(\delta)$ inside this region doesn't cause a bifurcation. For c real near $p(\gamma_-)$, there is a period two attractor which fails to attract the critical point; it is attracted to the saddle instead. As one leaves this region into region \mathfrak{g} , the saddle splits into a repelling fixed point and a period two saddle.

Region $\circ\bullet$ In this region, which is inside the main loop of the limaçon, we have one attractive and one repelling fixed point. When one enters this region from region $\circ+\mathfrak{g}$, one of the attracting points and the saddle collide and cancel. When one enters here from region $\circ+$, the saddle point merges with a period 2 attractor and an attracting fixed point is created. When one crosses into \mathfrak{g} , the attracting fixed point becomes repelling and typically a Hopf bifurcation occurs. We will discuss the direction of the Hopf bifurcation at the end of this section.

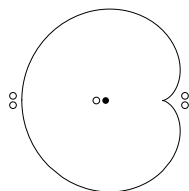


FIGURE 4.5: The types of fixed points occurring in the c -plane when the map is conformal ($\alpha = 1$). The labelling is as in Figure 4.4.

CASE $\alpha = 1$ (the conformal case, Figure 4.5): In this case the limaçon is a cardioid and $p(\gamma_{\pm})$ are points on the real axis.

Region $\circ\bullet$ Inside the cardioid there is one attracting and one repelling fixed point. As must occur in a conformal system, the attracting fixed point always attracts the critical point.

Region \mathfrak{g} Outside the cardioid there are two repelling fixed points. In this case, no Hopf bifurcation can occur; when going through a point on the cardioid for which the derivative at the fixed point is of the form $e^{2\pi ip/q}$, a Leau-Fatou flower bifurcation occurs. (See [M]).

CASE $\alpha > 1$ (Figure 4.6): In this case the limaçon is convex or has a dimple. In this case we conjecture (based on numerical evidence) that the critical point is attracted to the attractive point when it exists.

Region \mathfrak{g} Outside the limaçon and outside $p(\gamma_{\pm})$ there are two repelling fixed points.

Region $\mathfrak{g}+\bullet$ The limaçon cuts $p(\gamma_+)$ into four pieces. The two pieces intersecting the real line form region $\mathfrak{g}+\bullet$, which has two repelling fixed points, one attracting fixed point, and one saddle point. As for $\alpha < 1$, crossing $p(\delta)$ inside this region doesn't cause a bifurcation. When crossing $p(\gamma_+)$ into region \mathfrak{g} , the attracting fixed point and the saddle collide; crossing into region $\circ\bullet$ causes one of the repelling fixed points and the saddle to collide.

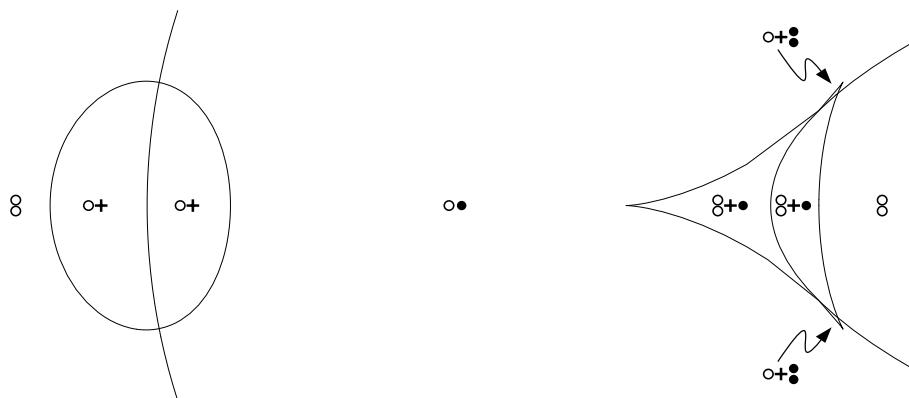


FIGURE 4.6: The types of fixed points occurring in the c -plane when $\alpha > 1$. As in Figure 4.4, the upper and lower pieces of the limaçon have been omitted, and the right-hand side has been greatly magnified.

- Region $o+•$: This very tiny region consists of the two components inside both $p(\gamma_+)$ and $p(\delta)$ which do not intersect the real line. Here there are 2 attracting fixed points, one repelling, and one saddle point. When moving from here to region $o•$ an attracting fixed point and a saddle cancel each other. When moving from here to region $8+•$, one of the attracting fixed points loses stability and becomes repelling, generally via a Hopf bifurcation.
- Region $o+$: Inside $p(\gamma_-)$, we have one saddle point and one repeller. As before, crossing $p(\delta)$ inside this region causes no bifurcation. When crossing into 8 , the saddle splits into a period two saddle and a repelling fixed point.
- Region $o•$: Inside the limaçon and outside $p(\gamma_{\pm})$, there is one attracting and one repelling fixed point. When one crosses $p(\gamma_+)$ from region $8+•$, one of the repelling fixed points and the saddle collide. When one crosses from region $o+$ to here an attracting period 2 orbit merges with the saddle to form an attracting fixed point.

We now give the analysis that leads to the bifurcation pictures above. We first consider the case where the parameter c is real.

PROPOSITION 4.7. *If c is real, the map $f_{\alpha,c}$ has at most four fixed points.*

Proof. The point $re^{i\theta}$ is a fixed point if

$$re^{i\theta} - r^{2\alpha}e^{2i\theta} = c.$$

Looking at the imaginary part, we see that

$$r \sin(\theta) - 2r^{2\alpha} \sin(\theta) \cos(\theta) = 0,$$

and so either $\sin(\theta) = 0$ or $r = 2r^{2\alpha} \cos(\theta)$. In the first case, there are two real solutions if c is less than c_0 , where $f_{\alpha,c_0}(x)$ is tangent to $y = x$. In the second case, we obtain $r^{2\alpha} = c$ after substituting into the real part of the original equation, and thus we get at most one value

for r . Substituting this value for r into the original equation gives a quadratic equation in $e^{i\theta}$ which has a solution for c greater than $c_1 < c_0$. \square

We can explicitly calculate the type of fixed points which occur on the real line: the only way the type of fixed points (or total number of fixed points) can change is by crossing one of the curves $p(\delta)$ or $p(\gamma_{\pm})$. Assuming these curves intersect as discussed earlier, the types of fixed point occurring in each region can be calculated by considering all possible bifurcations which can occur. We know that $p(\delta)$ is a limaçon. The difficult part of the analysis is then to figure out how the curves $p(\gamma_{\pm})$ cross the limaçon. First we show that $p(\gamma_-)$ intersects the limaçon as shown in the figures by showing that p is injective on the left half plane.

PROPOSITION 4.8. *The function p is injective on the left half plane.*

Proof. Observe that $p : \mathbb{C} \rightarrow \mathbb{C}$ is proper and surjective. Consequently, p maps closed sets to closed sets. Let \mathcal{L} denote the closed left half-plane:

$$\mathcal{L} = \{z \mid \operatorname{Re} z \leq 0\}.$$

Note that p maps the negative real axis onto itself and the imaginary axis onto a parabola-shaped curve which intersects only at the origin:

$$p(iy) = |y|^{2\alpha} + iy.$$

Since p has no singularities on \mathcal{L} , p is open and orientation preserving on \mathcal{L} . In particular, $p(\mathring{\mathcal{L}})$ is open. Since $p(\mathcal{L})$ is closed, we conclude that $p(\mathring{\mathcal{L}})$ is contained in the component of the complement of the image of the imaginary axis which contains the negative real axis. Thus $p(\mathcal{L})$ is the closure of this component, since $p(\mathcal{L})$ is closed. The map p is proper on \mathcal{L} , and maps \mathcal{L} onto this component, so the degree of p is well defined. Since $p^{-1}(0) = \{0\}$, this degree is one. We conclude that p maps the left half plane diffeomorphically onto the component described before. \square

We now consider $p(\gamma_+)$:

- *The image of the intersections of γ_+ and δ :* At these two points Dp has 0 as a double eigenvalue. These points can be explicitly computed, and one finds the rank there to be one. This explains the two points of tangency in the image of the two intersections.
- *The points where the tangent line to γ_+ is in the kernel of Dp :* One can calculate that there are exactly three such points, one of which is real (the point c_1 described in Proposition 4.7) and the other two are complex conjugates. This explains the three cusp points.
- *The points where the tangent line to γ_+ is horizontal or vertical:* One can calculate that there is only one point, c_1 , which has a horizontal tangency. When $\alpha < 2$ there is only one point (the point c_0 described in Proposition 4.7) at which $p(\gamma_+)$ has a vertical tangency.

Using the above one can show that $p(\gamma_+)$ intersects the limaçon as indicated in the pictures. It is not hard to show that $p(\gamma_+)$ and $p(\gamma_-)$ do not intersect.

Hopf Bifurcation. Consider a small disc D with center $c_0 \in \delta$ with Df_{c_0} having complex conjugate eigenvalues of absolute value 1 at one fixed point. We wish to discuss the bifurcation picture in this disc. For c in this disc, we can smoothly parametrize the corresponding fixed point $z(c)$, so that $z(c_0) = z_0$. When D is small enough this map $z : D \rightarrow \mathbb{C}$ is a diffeomorphism. In particular, $z(D)$ intersects δ and $D - \delta$ consists of two regions, one where the fixed point is attracting and one where the fixed point is repelling. On the boundary of these regions the fixed point is neutrally stable. One should in general expect a Hopf bifurcation. By a Hopf bifurcation, we mean that as c passes through the curve δ , the fixed point z_0 will change stability and an invariant circle will be created or destroyed (see [MM] or [D]). This behavior is more precisely described in terms of normal forms.

Assume that we have chosen z_0 so that its eigenvalues are non-resonant: not first, second, third, or fourth roots of unity. Then one can change coordinates [MM], depending smoothly on the parameter c , so that one obtains the following normal form for $f_{\alpha,c}$, for $c \in D$:

$$F_c(z) = \lambda_c z(1 + v_c |z|^2) + O(z^5)$$

Notice that the eigenvalue λ_c and the coefficient v_c depend also on α . The map $c \mapsto \lambda_c$ is a diffeomorphism on D and intersects the unit circle. The bifurcation theory for c near c_0 depends on $\operatorname{Re} v_{c_0}$, provided it does not vanish.

CLAIM 4.9. *Assume that the eigenvalue λ_{c_0} is non-resonant. Then:*

- *When $1/2 < \alpha < 1$, $\operatorname{Re} v_{c_0}$ is positive.*
- *When $\alpha = 1$, v_{c_0} vanishes.*
- *When $\alpha > 1$, $\operatorname{Re} v_{c_0}$ is negative.*

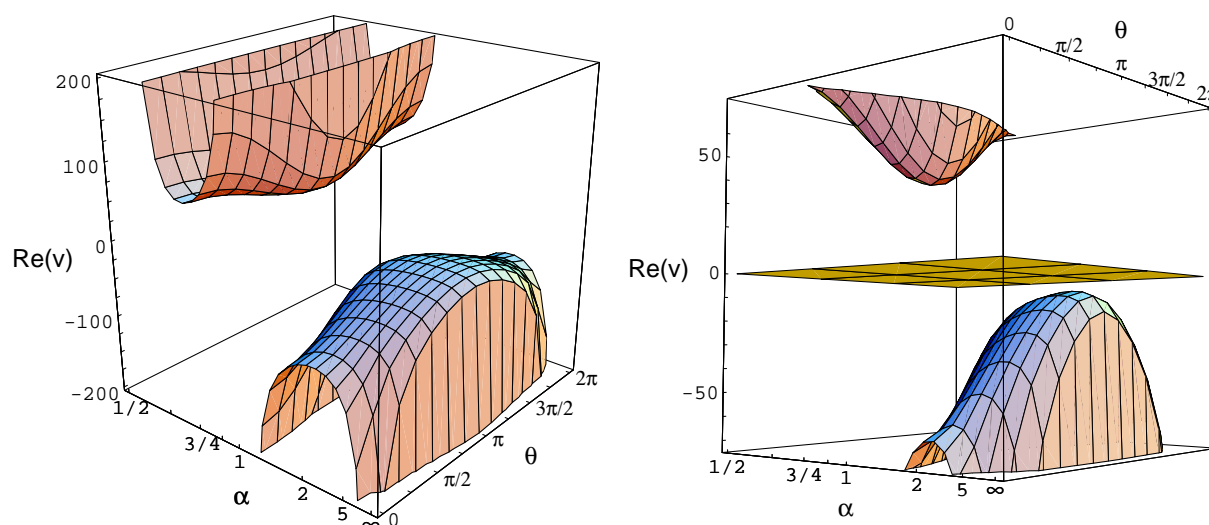


FIGURE 4.10: Graphs of $\operatorname{Re} v_{c_0}$ as a function of α and $\theta = \operatorname{Arg} \lambda_{c_0}$. We have modified the α scale so that the intervals $(\frac{1}{2}, 1)$ and $(1, \infty)$ have the same length. On the right is a closeup near the α - θ plane, which we have shaded to emphasize the claim.

Justification. When $\alpha = 1$, this is obvious. For any other values of α there seems to be no easy proof. The only more or less straightforward case is an infinitesimal computation near the holomorphic case $\alpha = 1$. Conceivably, a computer-assisted proof of this could be done using interval arithmetic. However, we feel this claim does not merit the effort of a difficult and tedious proof, and have used *Mathematica* [W] to perform the coordinate changes and compute v_{c_0} on a large grid of parameter values. See Figure 4.10. For $\alpha < 1$, we obtained (numerically) that $\operatorname{Re} v_{c_0} > 41.487$, and for $\alpha > 1$ that $\operatorname{Re} v_{c_0} < -8.594$. \square

By Claim 4.9, the sign of the real part of the coefficient v_{c_0} depends only on α , and hence we know in which direction the Hopf bifurcation occurs. Assuming that the disc D is small enough, we have the following dichotomy:

- When $\alpha < 1$ and $|\lambda_c| < 1$, there exists an invariant circle near $z(c)$ which is repelling in the normal direction. For λ_c outside the closed unit disc, there is no invariant circle near the point $z(c)$.
- When $\alpha > 1$, we have the opposite situation: for $|\lambda_c| < 1$, there is no invariant circle close to $z(c)$, and for λ_c outside the closed unit disc, there exists an invariant circle which is attracting in the normal direction. We conjecture that the critical point is still attracted to this circle.

5: Remarks on the Topology of the Connectedness Locus

In the holomorphic case ($\alpha = 1$), the connectedness locus is usually referred to as the Mandelbrot set, and is known to be connected [DH]; its complement in the Riemann sphere is conformally equivalent to the open disk. Furthermore, every connected component of its interior is a topological disk; these disks are referred to as either *hyperbolic components* or *queer components*. For any map lying within a hyperbolic component, there is a periodic attractor which necessarily attracts the critical point, and each hyperbolic component has a special point called the *center* (the parameter for which the critical orbit is periodic). Within any connected component of the interior of the Mandelbrot set, all maps except possibly one are topologically (in fact, quasi-conformally) conjugate; this exception is the center of a hyperbolic component.

A long standing conjecture is that there are no “queer components” in the Mandelbrot set; that is, all components of the interior are hyperbolic. This hyperbolicity conjecture is implied by the local connectivity of the Mandelbrot set (see [DH]). Yoccoz has shown that local connectivity holds for a “substantial” part of Mandelbrot set [Hu], and Swiatek [S], McMullen [McM], and Lyubich [Ly] have established the hyperbolicity conjecture along the real line by rather different techniques.

The situation when $\alpha \neq 1$ is quite different, as one should expect, because the iterates of the maps are not uniformly quasi-conformal. Douady and Hubbard’s proof that the Mandelbrot set is connected relies on the conformal structure; we see no way to adapt it to the non-conformal case. Furthermore, there is no mathematical relationship between the hyperbolicity conjecture and the local connectivity in this case. However, numerical evidence strongly suggests the following.

CONJECTURE 5.1. *For all $\alpha > 1/2$, the connectedness locus \mathcal{C}_α is connected. However, \mathcal{C}_α is not locally connected for all $\alpha \neq 1$.*

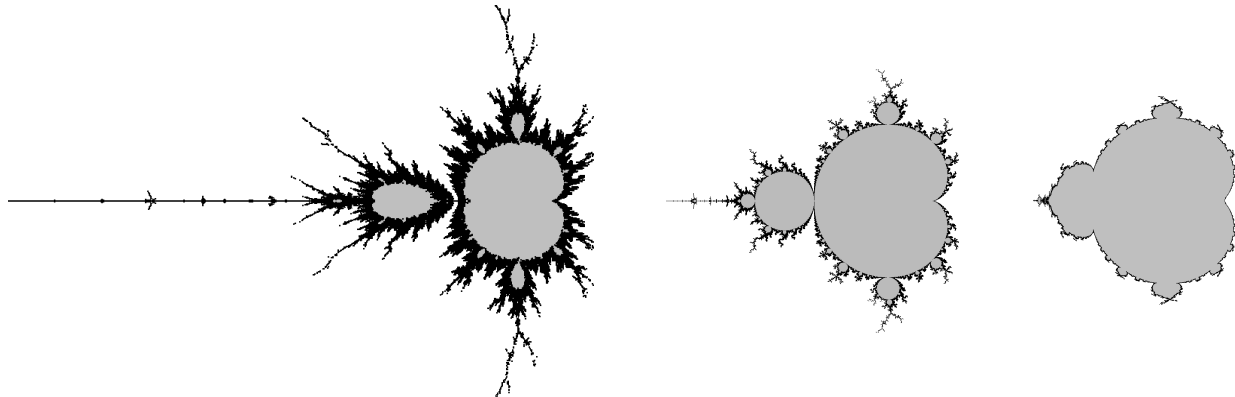


FIGURE 5.2: The connectedness loci \mathcal{C}_α for $\alpha = .75$, $\alpha = 1$, and $\alpha = 1.5$.

The apparent lack of local connectivity of \mathcal{C}_α in the non-conformal case is at least partially related to the presence of saddle points and their stable and unstable manifolds. Such invariant saddles make a qualitative understanding of the dynamics difficult and a quantitative understanding nearly impossible. In particular, when $\alpha < 1$, one can readily see the difficulty caused by the saddles.

Specifically, consider the interval of real parameters for which $f_{\alpha,c}|_{\mathbb{R}}$ has an attracting (in \mathbb{R}) fixed point which attracts the critical point. For some interval of parameters, this fixed point is not an attracting fixed point on \mathbb{C} , but is repelling in the imaginary direction (for example, in the region $\circ+$ discussed in section 4). Denote this fixed point by z_c and consider its global stable manifold $W^s(z_c)$. Because the dynamics is non-invertible, this global stable manifold is topologically more complicated than for a diffeomorphism. The critical point is in this stable manifold and one might hope that the filled-in Julia set is the closure of this stable manifold. Now consider a parameter value c' which is nearby, but not real. Consider the corresponding fixed point $z_{c'}$ and the corresponding global stable manifold. The critical point is not necessarily contained in this global stable manifold. In fact, the global stable manifold changes with the parameter; sometimes the critical point escapes to infinity and sometimes it is in $W^s(z_{c'})$. The detailed structure of the connectedness locus is unclear, but it has the topological appearance of a stable manifold. The rough structure of the \mathcal{C}_α for these parameters is that the main lobe (which contains those values of the c for which there is an attracting fixed point) is connected to the period two lobe, (containing those values for which there is an attracting cycle of period two) are connected only by a segment in the real line. A very complicated comb-like structure limits on part of this segment. See Figure 5.3.

When $\alpha > 1$, there is also an apparent lack of local connectivity near the real line, but in a dynamically different part of \mathcal{C}_α (for example, between the limit of period doubling and the creation of period 5 orbit; see Figure 5.3). At this point, we have no real understanding of what causes this, however.

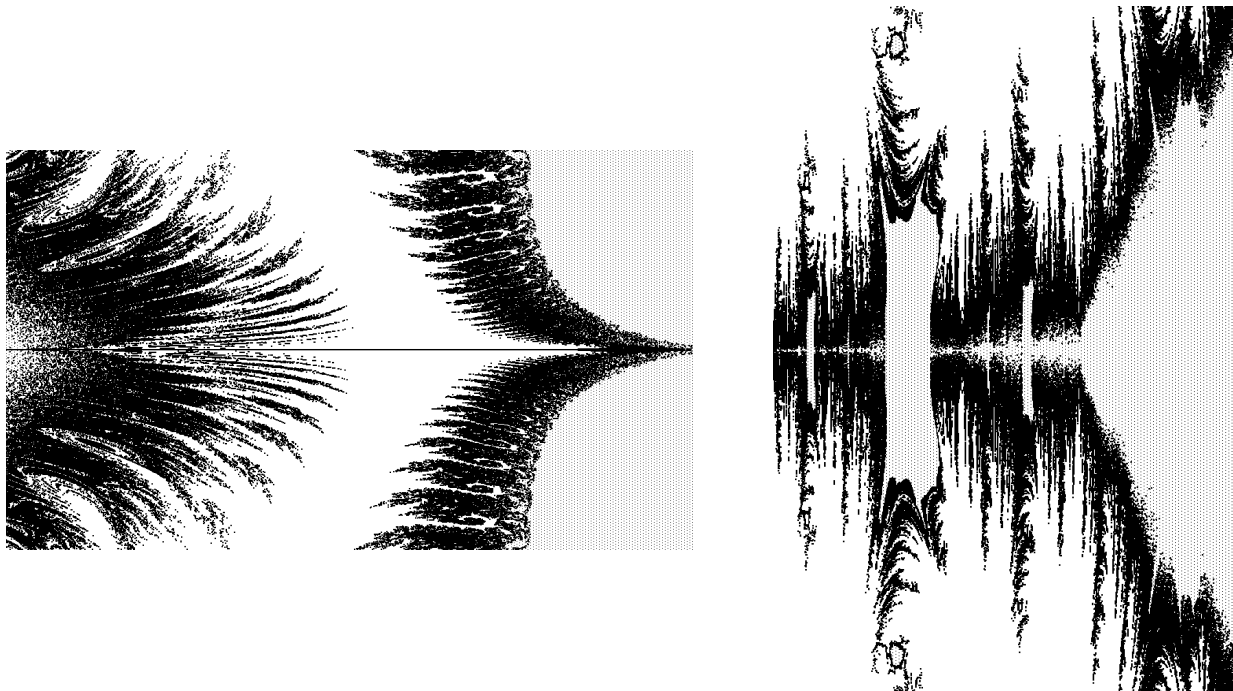


FIGURE 5.3: Blowups of the $\alpha = .75$ and $\alpha = 1.5$ connectedness loci showing the apparent lack of local connectivity.

Some insight into the topology of the boundary of the main lobe of \mathcal{C}_α can be gained by looking again at the Hopf bifurcation near the conformal case. We shall analyze the type of bifurcations which occur near parameters for which there is a fixed point of multiplier λ , where λ is a q^{th} root of unity ($q \geq 5$). We shall omit most of the tedious calculations here; the interested reader should refer to section 5 of [BSTV].

In this situation, one can change coordinates [MM] so that we have a two complex-parameter family of maps defined near the origin in the complex plane:

$$F_{\mu,a}(z) = \lambda z(e^\mu + a|z|^2 + z^q) + O(|az^4|, |a\mu z^3|, |\mu z^{q+1}|, |z^{q+2}|).$$

(Here $a \sim (1 - \alpha)/\lambda$.) We are interested in the q -periodic points of the map $F_{\mu,a}$; one easily sees that for such a point we have

$$z = z(e^{q\mu} + qa|z|^2 + qz^q) + O(|az^4|, |a\mu z^3|, |\mu z^{q+1}|, |z^{q+2}|).$$

We first consider the parameter a to be real, negative, small and fixed. (this corresponds to $\alpha > 1$.) When $\text{Re } \mu \leq 0$, the fixed point $z = 0$ is an attractor; the product of its eigenvalues is less than 1. When $\text{Re } \mu > 0$, the fixed point is repelling, but for $\text{Re } \mu$ sufficiently small, there exists an attracting, invariant (Hopf) circle whose diameter is of order $\sqrt{\frac{\text{Re } \mu}{|a|}}$. One can show that there is also a q -periodic orbit located approximately on the circle of radius $|a|^{\frac{1}{q-2}}$. When $|\mu|$ is small, it is easily seen that this orbit is repelling.

In a horn shaped domain in the μ -plane, the rotation number on the invariant circle is p/q (recall $\lambda = e^{2\pi ip/q}$); this horn is in fact the p/q -resonance horn or Arnol'd tongue [Ar,

ACHM, Ha]. Within this horn, there are two additional q -periodic orbits: one is a saddle and the other is an attractor; the invariant circle around the repelling fixed point is the closure of the unstable manifold of the p/q -saddle, which contains the attracting orbit. If μ leaves the horn “through the side”, i.e., fix $\operatorname{Re} \mu$ and vary $\operatorname{Im} \mu$, the saddle and the attractor collide, and although there is still an invariant circle, the rotation number is no longer $\operatorname{Arg} \lambda$. If instead we allow $\operatorname{Re} \mu$ to increase sufficiently, the saddle and the repeller collide, leaving a single attracting orbit of period q . However, before this collision occurs, the invariant circle loses smoothness and becomes only a topological circle. This loss of smoothness occurs when the eigenvalues of the p/q -sink become complex. See [ACHM, § 8].



FIGURE 5.4: The $2/5$ limb for $\alpha = 1.5$. The regions in grey indicate that the critical point converged to a periodic attractor of moderate (< 100) period within a few hundred iterations. Note the grey horn-like region at the base. The boundary of the figure appears disconnected due to the algorithm used to produce the picture; a different algorithm gives a much “thicker” boundary.

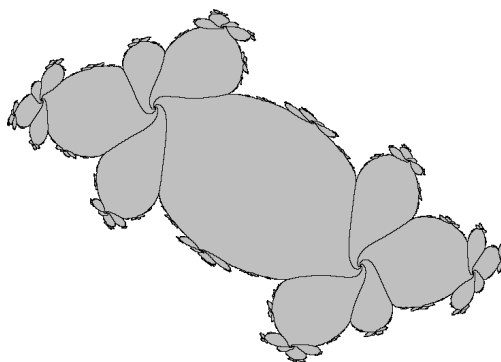


FIGURE 5.5: A Julia set for c within the $2/5$ resonance horn for $\alpha = 1.5$. The large grey areas are the basin of attraction of the $2/5$ attracting periodic orbit. This attracting orbit has complex eigenvalues, and so the unstable manifold of the $2/5$ periodic saddle does not form a smooth invariant circle. This saddle orbit lies on the five smooth curves which divide the grey regions; these curves are the stable manifold of the saddle.

Experimental evidence indicates that the critical orbit remains bounded for all parameter values discussed above: it is attracted to either the attracting fixed point ($\operatorname{Re} \mu < 0$), the invariant circle, or the p/q -periodic attractor. This gives some explanation for the appearance of the connectedness locus near the main lobe: the p/q -lobe sits at the end of a resonance horn, and is hence attached along an arc of values. See Figure 5.4.

When a is positive (corresponding to $\alpha < 1$), the picture is the other way around. As above, the fixed point is attracting for $\operatorname{Re} \mu < 0$ and repelling for $\operatorname{Re} \mu > 0$, but the invariant circle is repelling and exists only when $\operatorname{Re} \mu < 0$. Within a horn of μ values, the invariant circle contains a p/q -saddle and a p/q repeller, and is the closure of the stable manifold of the saddle. For all $\operatorname{Re} \mu$ negative and μ sufficiently small, there is another q -periodic orbit nearby, which is attracting.

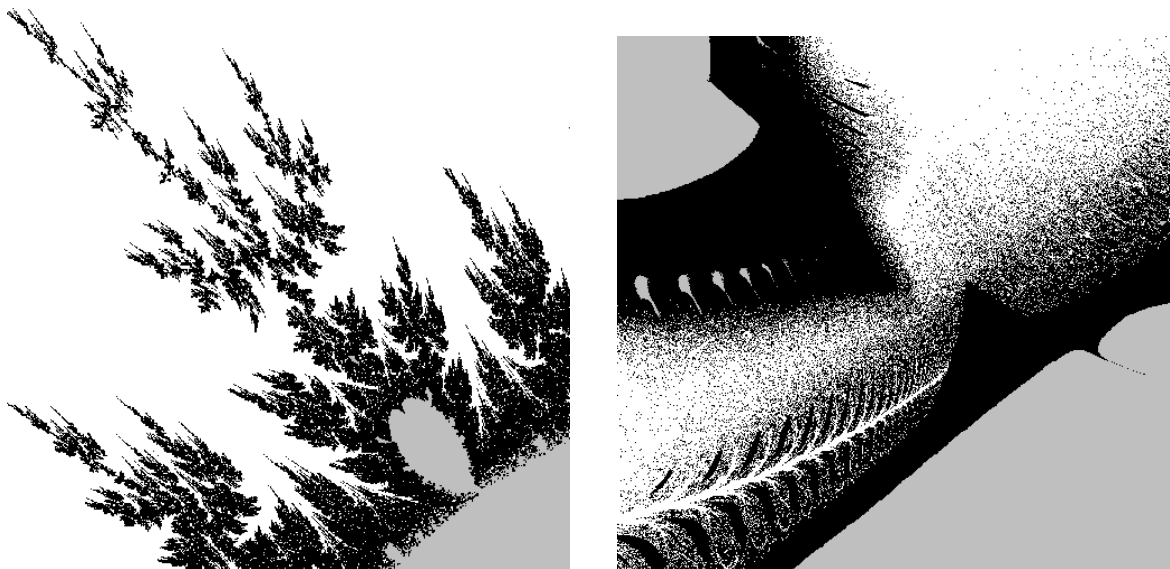


FIGURE 5.6: The $2/5$ limb for $\alpha = 0.75$, and a blowup (at right). The two figures were produced with different algorithms; in the left-hand picture, grey denotes parameters for which the critical point failed to escape within 256 iterations, while on the right such parameter values are colored black, and grey is used to indicate convergence of 0 to an attracting orbit of moderate period.

However, in this case the relationship between the Arnol'd tongue and the connectedness locus is quite different. Since the circle is repelling, for many parameter values in the horn, the critical orbit does not limit on the attracting fixed point; it can escape to ∞ , and hence the filled-in Julia set will be disconnected. Thus, one cannot readily detect the presence of the Arnol'd tongues from the connectedness locus alone, as in the case of $\alpha > 1$.

There is, however, a horn-like structure which is readily apparent along the boundary of \mathcal{C}_α . See Figure 5.6. This is related to the presence of q -periodic saddles. Near this horn, there are three period q orbits, as well as the attracting fixed point. Two of the periodic orbits are repelling, and the the other is a saddle. The horn corresponds to the parameter values for which the critical point lies between the one side of the stable manifold of a saddle point z and the other side of the stable manifold for its image $f_c(z)$. See Figure 5.7. At the point of the horn, a saddle connection occurs: one side of the local stable manifold of the periodic saddle z is the local unstable manifold for its image $f_c(z)$.

Attached to the top of the horn is a curve for which the critical orbit remains bounded, although it is not attracted to an attractor. For these parameters, the critical point lies on the stable manifold of one of the points of the period- q saddle orbit discussed above. This orbit appears to persist long enough to attach the period- q lobe (within which there is an attracting period q orbit) to the main lobe. Thus, \mathcal{C}_α is not disconnected as it appears in Figure 5.6.

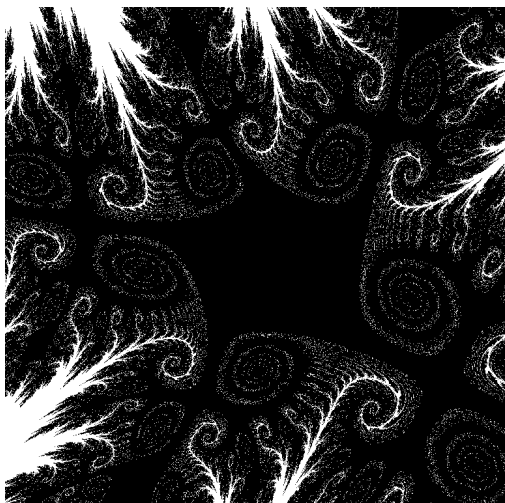


FIGURE 5.7: A close-up of the filled Julia set for $\alpha = .75$ and c within the horn in Figure 5.6. There is an attracting fixed point at the center of the picture, with a pair of period 5 repellers surrounding it (at the ends of the black and white spirals nearest the center), and a period 5 saddle at the edge of the large black region. The critical point, 0, lies in the large black cross shaped region near the lower right.

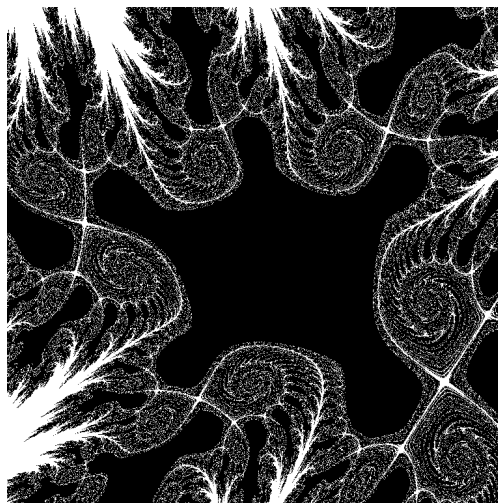


FIGURE 5.8: A close-up of the filled Julia set for $\alpha = .75$ and c just outside the horn in Figure 5.6. As in Figure 5.7, there is period 5 saddle, two period 5 repellers, and an attracting fixed point, in approximately the same locations. However, in this case the attractor fails to attract the critical point; 0 iterates to infinity, and the filled Julia set is disconnected, although not totally disconnected.

References

- [A] L. Ahlfors: *Lectures on Quasiconformal Mappings*. Wadsworth, 1987.
- [ACHM] D. Aronson, M. Chory, G. R. Hall, R. McGehee: Bifurcations from an Invariant Circle for Two-Parameter Families of Maps of the Plane: A Computer-Assisted Study. *Comm. Math. Phys.* **83** (1982), 303–354.
- [Ar] V. I. Arnol'd: Small Denominators I. On the Mappings of the Circumference of the Circle onto Itself. *Translations Am. Math. Soc., 2nd series* **46** (1965), 213–284.
- [BSTV] B. Bielefeld, S. Sutherland, F. Tangerman, and J.J.P. Veerman: *Dynamics of Certain Non-Conformal Degree Two Maps of the Plane*. Stony Brook Institute for Math. Sciences preprint #1991/18.
- [Bl] P. Blanchard: Complex Analytic Dynamics on the Riemann Sphere, *Bull. Amer. Math. Soc.* **11** (1984), 85-141.
- [D] R. Devaney: *An Introduction to Chaotic Dynamical Systems*, 2nd ed. Addison-Wesley, 1989.
- [DH] A. Douady, and J. Hubbard: *Etude Dynamique des Polynômes Complexes I, II*, Publications Mathématiques d'Orsay **84–02** (1984), and **85–04** (1985).

- [Ha] G. R. Hall: Resonance Zones in Two-Parameter Families of Circle Homeomorphisms, *SIAM J. Math. Anal.* **15** (1984), 1075–1081.
- [HPS] M. Hirsch, C. Pugh, and M. Shub, *Invariant Manifolds*, Lecture Notes in Mathematics, Vol. 583. Springer-Verlag, 1977.
- [Hu] J.H. Hubbard: Local Connectivity of Julia Sets and Bifurcation Loci: Three Theorems of J.-C. Yoccoz, pp. 467–511 in *Topological Methods in Modern Mathematics, A Symposium in Honor of John Milnor's 60th Birthday*, Publish or Perish, 1993.
- [J1] Y. Jiang, Generalized Ulam-von Neumann Transformations, Thesis, CUNY Graduate Center, 1990.
- [J2] Y. Jiang, Dynamics of Certain Nonconformal Semigroups, *Complex Variables* **22** (1993), 27–34.
- [L] O. Lehto, *Univalent Functions and Teichmüller Spaces*. Springer-Verlag, 1987.
- [Ly] M. Lyubich, *Geometry of Quadratic Polynomials: Moduli, Rigidity and Local Connectivity*, Stony Brook Institute for Math. Sciences preprint #1993/9.
- [McM] C. McMullen, *Complex Dynamics and Renormalization*, preprint, U.C. Berkeley Math. Dept., 1993.
- [MSS] R. Mañé, P. Sad, and D. Sullivan, On the Dynamics of Rational Maps, *Ann. Scient. Éc. Norm. Sup.*, 4^e série, **16** (1983), 193–217.
- [MM] J. Marsden and M. McCracken, *The Hopf Bifurcation and its Applications*. Springer-Verlag, 1976.
- [M] J. Milnor, *Dynamics in One Complex Variable: Introductory Lectures*, Stony Brook Institute for Math. Sciences preprint #1990/5.
- [S] G. Świątek, *Hyperbolicity is Dense in the Real Quadratic Family*, Stony Brook Institute for Math. Sciences preprint #1992/10.
- [W] S. Wolfram, *Mathematica: A System for Doing Mathematics by Computer*, Addison-Wesley, 1988.